Proceedings of the Combustion Institute, Volume 29, 2002/pp. 973–980

SUM-FREQUENCY GENERATION *IN SITU* STUDY OF CO ADSORPTION AND CATALYTIC CO OXIDATION ON RHODIUM AT ELEVATED PRESSURES

T. PERY,[1] M. G. SCHWEITZER,[1] H.-R. VOLPP,[1] J. WOLFRUM,[1]
L. CIOSSU,[2] O. DEUTSCHMANN[2] AND J. WARNATZ[2]

[1]*Physikalisch Chemisches Institut*
Universität Heidelberg
Im Neuenheimer Feld 253
D-69120 Heidelberg, Germany
[2]*Interdisziplinäres Zentrum für Wissenschaftliches Rechnen*
Universität Heidelberg
Im Neuenheimer Feld 368
D-69120 Heidelberg, Germany

Optical IR-visible sum-frequency generation surface vibrational spectroscopy was employed for *in situ* detection of chemisorbed CO during CO adsorption and catalytic CO oxidation on a rhodium (111) catalyst in the substrate temperature range T_s = 300–800 K. CO adsorption studies performed over 12 orders of magnitude in CO pressure (p_{CO} = 10^{-8}–1000 mbar) demonstrated the reversible molecular adsorption of CO up to a pressure of about 10 mbar. For CO pressures above 10 mbar, the onset of a new irreversible dissociative CO adsorption pathway could be observed already at a substrate temperature of T_s = 300 K. CO dissociation was found to result in the formation of carbon on the surface as the only detectable dissociation product, indicating that CO dissociation occurs via the Boudouard reaction: $2CO \rightarrow C(s) + CO_2$. Further experiments were performed to investigate catalytic oxidation of CO under intermediate reagent pressure conditions (p_{tot} = 20 mbar). The latter experiments were performed under laminar flow conditions in a well-defined stagnation point flow geometry to allow for comparison with numerical reactive flow simulations based on a detailed Langmuir-Hinshelwood (LH) surface reaction mechanism for CO oxidation, including molecular adsorption and desorption of CO and dissociative adsorption of oxygen as well as the formation of CO_2 through reaction of the adsorbed CO and O species. The good agreement obtained between the results of the CO oxidation experiment and the simulation indicates that for CO and O_2 partial pressures as typically present in the exhaust gas of spark-ignited internal combustion engines, the Rh(111)-catalyzed CO oxidation can be quantitatively described in the framework of a mean-field approach employing an LH reaction scheme along with kinetics data derived in surface science studies.

Introduction

Rhodium represents one of the most important catalyst constituents in many industrial processes, such as CO methanation and Fischer-Tropsch synthesis [1,2]. Because of its high efficiency in catalyzing the reduction of NO to N_2 and the oxidation of CO to CO_2, Rh is an essential component of commercial three-way automobile catalytic converters [3]. As a consequence, the adsorption of CO on Rh has been investigated quite extensively under ultrahigh vacuum (UHV) conditions [4,5].

However, only a few studies have been reported so far in which CO adsorption on Rh was investigated under actual high-pressure conditions. In recent experiments, optical IR-visible sum-frequency generation (IR-VIS SFG) [6,7] and scanning tunneling microscopy (STM) [8] were employed for *in situ* studies of CO adsorption on an Rh(111) catalyst at room temperature up to a CO pressure of 1000 mbar. The SFG studies demonstrated the appearance of new "low-frequency" CO stretching vibrational features, which could not be observed in previous studies under UHV conditions [6,7]. The new spectral features were assigned to CO molecules terminally adsorbed on defect sides, which were proposed to result from pressure-induced surface roughening of the Rh(111) surface [6]. In Ref. [6], it was further proposed that this process is reversible with respect to CO pressure variation. However, subsequent SFG studies indicated that high CO pressures of about 900 mbar may cause irreversible changes in the Rh(111) surfaces [7]. To shed more light on the actual CO adsorption mechanism, in the present work experiments were carried out in which IR-VIS SFG for *in situ* CO detection in the pressure range p_{CO} = 10^{-8}–1000 mbar was combined with "postreactive" Auger electron spectroscopy (AES) studies of the Rh(111) surface. With such an experimental approach, the occurrence of a

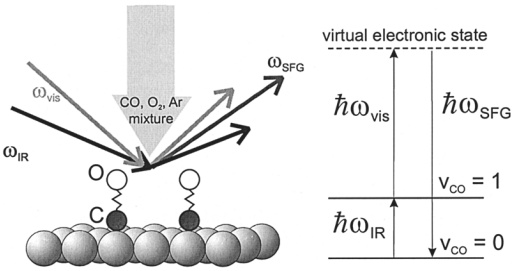

FIG. 1. (a) Schematic illustration of second-order nonlinear optical IR-VIS SFG which was applied in the present study for the *in situ* detection of CO adsorbed on an Rh(111) single-crystal catalyst. (b) Energy-level diagram of the vibrationally resonant IR-VIS SFG process, which allows for surface vibrational spectroscopy of adsorbed CO species.

new high-pressure and high-temperature dissociative CO adsorption pathway has been recently revealed for the CO/Pt(111) system [9,10].

In the present work, this experimental approach was further applied to study heterogeneous CO oxidation on Rh(111) at a CO partial pressure of 2 mbar, as typically present in the exhaust gas of a spark-ignited internal combustion (IC) engine. For comparison with the experimental results, a numerical simulation of the reactive flow system corresponding to the conditions of the experiment was performed, including detailed submodels for molecular transport and surface chemistry.

Experimental

Experiments were carried out in a reaction chamber, which allows catalytic studies starting from UHV conditions (base pressure $\sim 3 \times 10^{-10}$ mbar) up to atmospheric pressure. In the elevated pressure regime ($\geq$1 mbar), the experimental arrangement can be utilized to investigate reactive processes for well-defined stagnation point flows on catalytic surfaces [11,12]. The chamber was equipped with a quadrupole mass spectrometer (QMS) for thermal-programmed desorption (TPD) measurements, an Ar^+-ion sputter source, a four-grid retarding field analyzer for AES and low-energy electron diffraction (LEED) measurements. A second differentially pumped QMS was connected to the exhaust-gas line for on-line monitoring of the stable reaction product CO_2 [11]. The Rh catalyst (9 mm diameter Rh(111) single-crystal disk, purity 99.99%) could be resistively heated in the substrate temperature range T_s = 300–1600 K. A clean Rh surface was obtained by applying several cycles of Ar^+-ion sputtering followed by oxidation at 1000 K. After the cleaning procedure, residual oxygen was removed and surface order was restored by annealing the crystal at 1400 K.

For the SFG measurements, a 40 ps mode-locked Nd:YAG laser system was used. A part of its output was frequency doubled to 532 nm and used as the visible input for the SFG process. The other part was used to pump an optical parametric system to generate IR radiation tunable in the frequency range ω_{IR} = 1800–2200 cm^{-1} with a pulse duration of 25 ps. The IR laser frequency was calibrated to an absolute accuracy of ± 1 cm^{-1} by measurements of the gas-phase CO absorption bands around 2143 cm^{-1} in a reference cell. The visible and IR laser beams were overlapped at the surface, and the SFG signal reflected from the Rh surface was detected by a photomultiplier (Fig. 1). SFG is a second-order nonlinear optical process where a tunable IR (ω_{IR}) laser beam is mixed with a visible (ω_{VIS}) laser beam to generate a sum-frequency output (ω_{SFG}) which is highly specific to the interface region [13]. When the IR beam is tuned over a vibrational resonance of a surface species, the effective surface nonlinear susceptibility is resonantly enhanced and a vibrational spectrum of surface species can be measured [14].

Results and Discussion

Pressure Dependence of CO Adsorption (p_{CO} = 10^{-8}–1000 mbar)

Figure 2 depicts SFG spectra recorded in the CO pressure range 10^{-8}–1000 mbar together with an SFG spectrum obtained after the pressure was reduced to 10^{-6} mbar. Comparison of the latter spectrum with the one obtained at the same CO pressure in the increasing pressure cycle clearly indicates the non-reversibility of the adsorption process. All spectra shown in Fig. 2 are dominated by a single vibrational feature with CO stretching frequencies in the range ω_{CO} = 2053–2075 cm^{-1}, typical for terminally bound CO on top of one rhodium surface atom [5]. Further detailed inspection of the spectra (see, e.g., in Fig. 2 the spectra recorded at 500 mbar) revealed a vibrational signal at a frequency of 1899 $\pm$ 4 cm^{-1} originating from CO bound to threefold coordinated hollow sites [5]. The observation of both on-top and hollow-site CO is consistent with the high-pressure Rh(111) + (2 $\times$ 2)-3CO (θ_{CO} = 0.75 ML) adsorbate structure derived in the recent STM studies [8]. One monolayer (ML) equals the number of rhodium atoms in the Rh(111) surface plane (1.60×10^{15} atoms/cm^2). However, due to the reduced sensitivity of SFG for the detection of multiple coordinated CO surface species [15], the relative SFG signal intensities do not reflect the actual on-top versus hollow-site CO coverage ratio of 1:2

of the Rh(111) + (2 × 2)-3CO (θ_{CO} = 0.75) adsorbate structure [5].

The relative on-top CO adsorbate density, $n_{ontop\text{-}CO}$, derived from the integrated vibrational band intensity is plotted in Fig. 3a against the CO pressure along with frequency values (Fig. 3b) obtained from the line shape analysis of the on-top CO vibrational bands. For comparison, the pressure dependence of the CO equilibrium surface coverage θ_{CO} is also depicted in Fig. 3c. The variation of the on-top CO adsorbate density with CO pressure and CO equilibrium surface coverage θ_{CO} is in agreement with previous LEED [5] and STM studies [8]. The latter measurements revealed a coverage-dependent shift in the CO adsorption site population from one where all CO molecules are adsorbed at on-top sites (for θ_{CO} = 1/3 and below) to one in which CO is adsorbed at on-top and threefold hollow sites with a ratio of 1:3 (for θ_{CO} around 0.57) and finally to one where CO occupies on-top and threefold hollow sites with a ratio of 1:2 (at the CO saturation coverage of 0.75).

The results depicted in Fig. 3b show that when the pressure is increased, the on-top CO stretching vibrational frequency is blueshifted from a value of 2053 ± 2 cm^{-1} at $p_{CO} = 10^{-8}$ mbar to value of 2075 ± 2 cm^{-1} for $p_{CO} = 10^{-2}$ mbar. In Ref. [6], the observed blueshift was attributed to an increase in the CO-CO vibrational coupling with increasing CO surface coverage (see Fig. 3c). If the CO pressure is further increased, the frequency remains almost constant in the pressure range $p_{CO} = 10^{-3}$–100 mbar, indicating that due to the strong repulsive interaction between the adsorbate molecules, the maximum CO coverage cannot be significantly altered after saturation coverage has been reached (see Fig. 3c). For higher pressures (p_{CO} > 100 mbar), however, the frequency decreases, finally reaching a value of ω_{CO} = 2065 ± 3 cm^{-1} at p_{CO} = 1000 mbar. The observed decrease of the on-top CO frequency above p_{CO} = 100 mbar, which is accompanied by an irreversible decrease of the on-top CO adsorbate density (see Fig. 3a), along with the presence of a considerable carbon signal observed in the "postreactive" Auger spectrum indicated the appearance of a new dissociative high-pressure CO adsorption mechanism (see below).

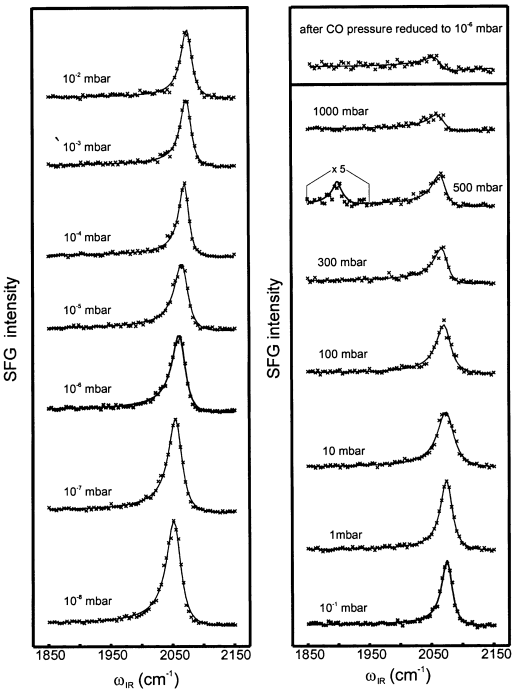

FIG. 2. SFG spectra of CO terminally adsorbed on the Rh(111) single crystal obtained in one single increasing CO pressure cycle in the range $p_{CO} = 10^{-8}$–1000 mbar at a substrate temperature of T_s = 300 K. Spectra were recorded under adsorption/desorption equilibrium conditions by tuning the IR laser over the frequency region ω_{IR} = 1850–2150 cm^{-1}, in which stretching vibrations of adsorbed CO species can be excited. For comparison, an SFG spectrum recorded after the CO pressure was reduced again to $p_{CO} = 10^{-6}$ mbar is shown in the upper right part of the figure. All spectra were normalized to the actual intensity of the IR laser beam at the Rh substrate in order to account for the different absorption of the IR laser radiation by the CO gas phase. The solid lines represent results of numerical simulations of the experimental spectral line shapes which were employed to derive the integrated vibrational band intensity and the stretching vibrational frequency, ω_{CO}, of the on-top adsorbed CO surface species (for details see, e.g., [14]).

Substrate Temperature Dependence of CO Adsorption

To study the temperature dependence of the CO adsorption on Rh(111), SFG spectra were recorded in the substrate temperature range T_s = 300–800 K for CO pressures in the range 10^{-8}–100 mbar. In the pressure range 10^{-8}–10^{-4} mbar, adsorbed CO could be detected up to T_s = 600 K, without any indication for dissociation. All SFG spectra could be well described by a single vibrational resonance originating from on-top adsorbed CO species (see Fig. 4a). At higher pressures (p_{CO} = 1 mbar) and substrate temperatures, however, an additional low-frequency vibrational feature which marks the onset of irreversible CO adsorption became observable, as can be seen in Fig. 5a. The dissociative adsorption of CO at higher substrate temperatures is demonstrated by the SFG and Auger electron (AE) data reproduced in Fig. 6.

The SFG spectrum shown in Fig. 6a was recorded

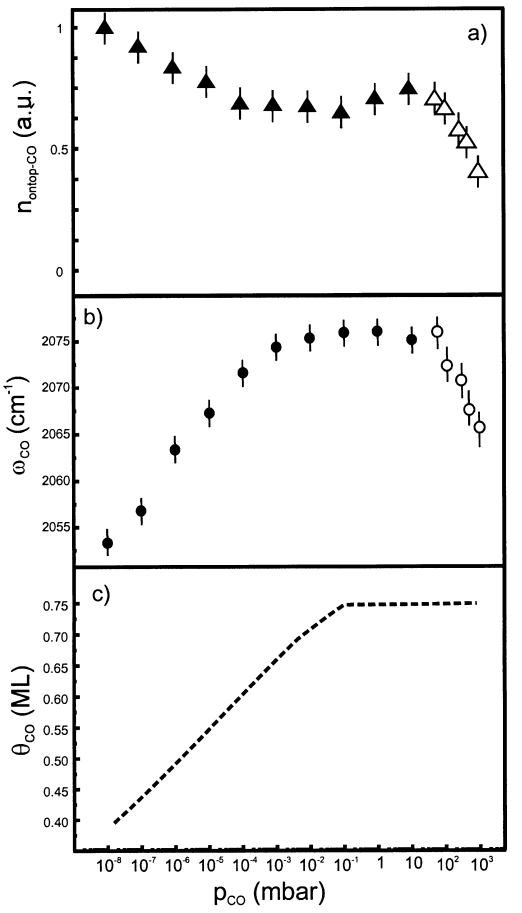

FIG. 3. (a) Relative on-top CO adsorbate density, $n_{ontop\text{-}CO}$, derived from the integrated vibrational band intensity of the SFG spectra shown in Fig. 2. In the determination of $n_{ontop\text{-}CO}$, it was taken into account that the integrated SFG intensity is proportional to the square of the ontop CO adsorbate density [15]. (b) Stretching vibrational frequency, ω_{CO}, of the ontop adsorbed CO molecules. The open symbols in (a) and (b) indicate the pressure range in which irreversible CO adsorption occurs. (c) CO equilibrium surface coverage, θ_{CO}, calculated using the adsorption/desorption kinetics data for molecular adsorption of CO on Rh(111) given in Table 1. Values are plotted against the CO gas-phase pressure.

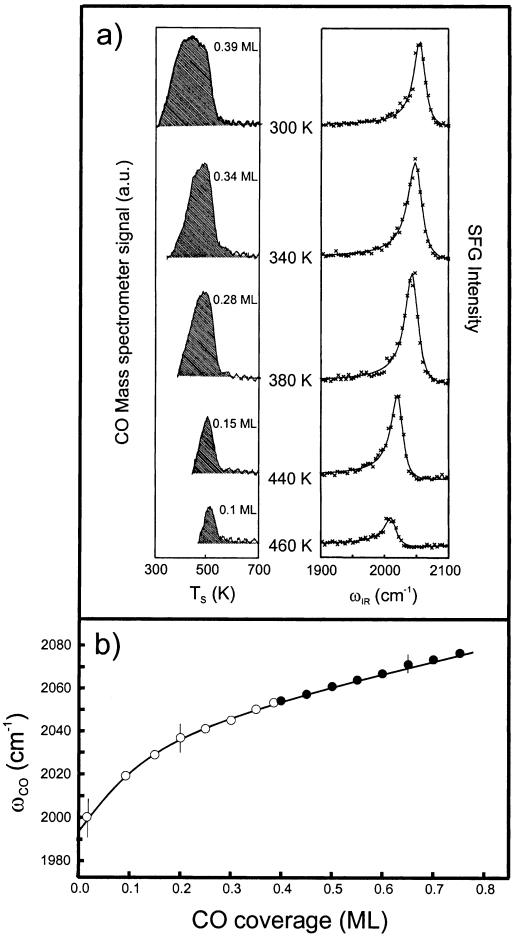

FIG. 4. (a) Right side: Typical SFG spectra of on-top CO surface species on Rh(111) recorded at different substrate temperatures at a fixed CO pressure of 10^{-8} mbar. The SFG intensity is plotted versus the frequency of the tunable IR laser. Experimental data points are represented by crosses, and solid lines represent results of numerical simulations of the experimental spectral line shapes used to determine the coverage dependence of the on-top CO stretching vibrational frequency ω_{CO}. Left side: TPD spectra of CO measured under molecular flow conditions at a CO pressure of 10^{-8} mbar. TPD spectra were recorded right after the corresponding SFG measurements (shown on the right side) were obtained. Desorption was started at different substrate temperatures as indicated in the figure. The surface coverages given in the figure were derived from the integrated areas of the TPD spectra and normalized to the value at the saturation coverage (θ_{CO} = 0.39 ML) at 300 K (for details, see [11]). (b) Coverage dependence of the stretching vibrational frequency, ω_{CO}, of the on-top adsorbed CO molecules. Open circles represent values derived from combined SFG and TPD measurements as illustrated in (a). Filled circles represent results of room-temperature adsorption studies carried out in the CO pressure range p_{CO} = 10^{-8}–10 mbar for which reversible molecular adsorption of CO occurs (see text and Fig. 2).

at a CO pressure of 1 mbar at T_s = 300 K. The spectrum depicted in Fig. 6b was obtained after the substrate temperature was increased to 680 K. In this case, the lower SFG intensity predominately reflects the fact that with increasing substrate temperature the equilibrium CO coverage decreases, which also explains the observed redshift of the center frequency of the on-top CO stretching vibrational band. Nevertheless, a second feature on the

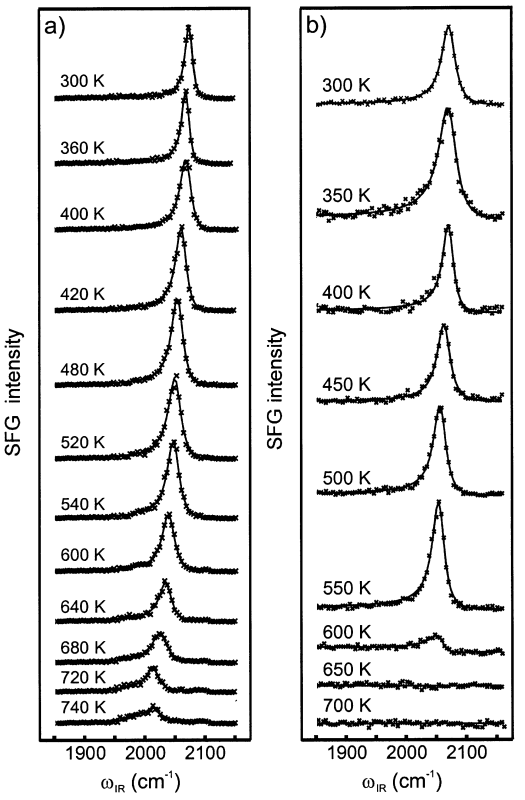

FIG. 5. (a) SFG spectra of CO terminally adsorbed on Rh(111) recorded at different substrate temperatures at a constant CO pressure of 1 mbar. The appearance of an additional low-frequency vibrational feature for substrate temperatures $T_s \geq 600$ K marks the onset of a new nonreversible dissociative CO adsorption mechanism (for details, see text). (b) SFG spectra of CO terminally adsorbed on Rh(111) recorded during CO oxidation under laminar flow conditions at a total pressure of 20 mbar in a stagnation point flow (CO, 15 sccm; O_2, 30 sccm; Ar, 105 sccm; flow velocity 2.5 cm/s). Experimental data points are represented by crosses, and the solid lines represent results of numerical simulations of the experimental spectral line shapes used to determine on-top CO stretching vibrational frequency ω_{CO} [14]. In the CO oxidation measurements, Ar was employed as in inert buffer gas and as an internal standard for the mass spectrometric determination of the CO_2 production rate shown in Fig. 7b (for details, see Ref. [11]).

low-frequency side of the on-top CO vibrational band is already noticeable. Fig. 6c finally shows an "SFG spectrum," recorded for $T_s = 680$ K after the CO pressure was raised to 100 mbar, in which no vibrational resonant signal can be discerned anymore. Comparison of the postreactive AE spectrum (Fig. 6c) with the one of the clean Rh surface (Fig. 6a) demonstrates that considerable amounts of

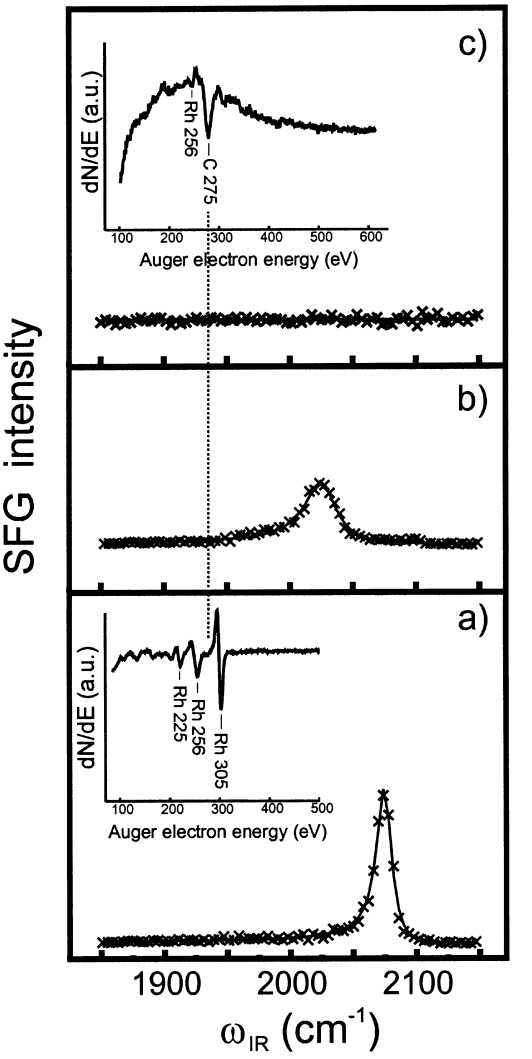

FIG. 6. (a) SFG spectrum of on-top adsorbed CO recorded at a CO pressure of 1 mbar and a substrate temperature of 300 K. The AE spectrum of the clean surface measured before the Rh substrate was exposed to CO is depicted as an insert. (b) SFG spectrum obtained after the substrate temperature was increased to $T_s = 680$ K. (c) An "SFG spectrum," recorded for $T_s = 680$ K after the CO pressure was raised to 100 mbar, in which no vibrational resonant signal could be discerned anymore. The fact that also after reducing the substrate temperature no noticeable vibrational resonant signal in the SFG spectra reappeared confirmed the irreversibility of the CO adsorption process under these pressure and temperature conditions. The AE spectrum of the Rh surface measured after the substrate temperature was reduced to 300 K and after evacuation of the reaction chamber down to about 10^{-9} mbar is depicted as an insert. Comparison of the latter postreactive AE spectrum with the one of the clean Rh surface shown in (a) demonstrates that considerable amounts of surface carbon, C(s), are deposited during the high-temperature and high-pressure adsorption of CO (for details, see text).

surface carbon, C(s), are deposited during "high-temperature" and "high-pressure" dissociative adsorption of CO. The fact that in contrast to most recent CO dissociation studies on Pt(111) [10], no oxygen signal was observed in the postreactive AE spectrum indicates that on Rh(111) the dissociation of CO proceeds predominately via the exothermic Boudouard reaction: $2CO \rightarrow C(s) + CO_2$. The downshift in the CO on-top stretching frequency observed in the present and in the previous [7] room-temperature CO adsorption studies for CO pressures ≥100 mbar (Fig. 3a) and the appeareance of a new low-frequency vibrational feature for substrate temperatures $T_s \geq 600$ K (see Fig. 5a) is due to the formation of on-top CO coadsorbed with carbon on the surface rather than due to a reversible adsorbate-induced surface roughening, as was tentatively proposed in Ref. [6].

CO Oxidation

SFG spectra recorded during CO oxidation are depicted in Fig. 5b. The spectra were evaluated using the CO frequency versus CO coverage curve depicted in Fig. 4b to determine the total CO coverage as a function of substrate temperature, as depicted in Fig. 7a. The CO_2 production rate simultaneously measured using mass spectrometry is reproduced in Fig. 7b. Postreactive AE spectra revealed that only trace amounts of surface carbon and Rh surface oxides are formed during CO oxidation under the present reagent pressure and substrate temperature conditions. The formation of Rh surface oxides, which results in an efficient deactivation of the catalyst surface, has been observed in previous CO oxidation studies on Rh(111) for oxygen partial pressures of about 500 mbar [16].

As can be seen in Fig. 7a, the presence of O_2 in the stagnation flow does not result in a reduction of the CO surface coverage, indicating that adsorbed CO efficiently blocks the adsorption of oxygen up to a substrate temperature of about 400 K [16]. Only for temperatures above $T_s = 400$ K does the CO coverage start to decrease from the saturation value of $\theta_{CO} = 0.75$. At the same time, the onset of CO_2 production becomes noticeable, as indicated by the results shown in Fig. 7b. In the temperature range $T_s = 400$–600 K, the CO equilibrium coverage decreases linearly with substrate temperature. In this temperature range, the rate-determining step for CO_2 production is the dissociative adsorption of O_2, which is hindered by the high CO surface coverage [16]. The sudden decrease in CO coverage at $T_s > 600$ K in Fig. 7a is due to a transition from a predominately CO-covered surface state to an O-covered state originating from an increase of dissociative oxygen adsorption with decreasing CO coverage and the increase of the surface reaction rate.

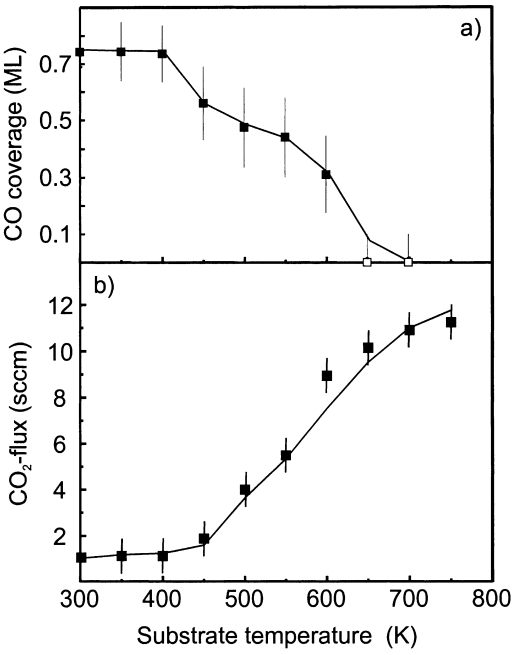

FIG. 7. (a) CO surface coverage (filled squares) as a function of the Rh(111) substrate temperature obtained during CO oxidation. (b) CO_2 production rate simultaneously measured using mass spectrometry. Measurements were performed at a total pressure of 20 mbar under laminar flow conditions in a stagnation point flow (CO, 15 sccm; O_2, 30 sccm; Ar, 105 sccm; flow velocity 2.5 cm/s). The solid lines in (a) and (b) represent the results of a numerical simulation corresponding to the conditions of the experiment. Details of the surface reaction mechanism are given in the text and in Table 1.

The solid lines depicted in Fig. 7a and 7b represent the results of a numerical simulation based on the model of a reactive stagnation point flow directed toward a reactive surface [12]. The surface processes are described by a mean-field (MF) model [17]. The surface reaction mechanism employed is based on a Langmuir-Hinshelwood (LH) scheme for CO oxidation, which includes molecular adsorption and desorption of CO, dissociative adsorption of molecular oxygen, as well as the formation of CO_2 through reaction of the adsorbed CO and O species (Table 1). In the surface reaction model, it was assumed that the oxygen sticking probability depends on the actual CO surface coverage, decreasing rapidly from an initial value of 0.9 in the limit of zero CO coverage [18,19] to about 1% of this value at $\theta_{CO} = 0.3$. The latter behavior of the oxygen sticking probability reflects the reduced availability of adjacent free adsorption sites for oxygen adsorption as a result of the repulsive interaction between the CO adsorbate molecules [16].

TABLE 1
Surface reaction mechanism and kinetic parameters for the oxidation of CO on Rh(111)

Reaction	ν_0 (s^{-1})	ν_1 (s^{-1})	E_0 (kcal/mol)	E_1 (kcal/mol)	S_0	Ref.
O_2 adsorption					0.9	[18,19]
O_2 desorption	3×10^5		24			[20]
CO adsorption					0.8	[21]
CO desorption	1.33×10^{14}	1.0×10^{10}	32.3	18.3		[21]
CO_2 production	1×10^{12}		25.3			[16,22]

Note: ν_0 and ν_1 (E_0 and E_1) are the pre-exponential factors (activation energies) for an isolated molecule and for a molecule at saturation coverage, respectively.

Conclusions

The present CO adsorption studies demonstrated reversible molecular adsorption of CO on Rh(111) up to a pressure of 10 mbar. For CO pressures above 10 mbar, the onset of a new irreversible dissociative CO adsorption mechanism on Rh(111) could be observed beginning at a substrate temperature of 300 K. At this temperature, as well in the substrate temperature range 600–800 K, CO dissociation was found to result in the formation of carbon on the surface as the only detectable dissociation product, indicating that CO dissociation on Rh(111) occurs via the Boudouard reaction: $2CO \rightarrow C(s) + CO_2$. The good agreement which could be obtained between the results of CO oxidation experiments and numerical simulations for CO and O_2 partial pressures as typically present in the exhaust gas of spark-ignited IC engines demonstrated that under these conditions, Rh(111)-catalyzed CO oxidation can be quantitatively described in the framework of a MF approach employing an LH surface reaction scheme which involves the reaction of adsorbed CO molecules with chemisorbed atomic oxygen species.

Acknowledgments

This work was supported by the Deutsche Forschungsgemeinschaft (DFG) within the Sonderforschungsbereich 359. HRV thanks G. Rupprechter (Chemical Physics Department, Fritz-Haber-Institut der Max-Planck-Gesellschaft, Berlin) for many helpful communications.

REFERENCES

1. Ertl, G., Knözinger, H., and Weitkamp, J. (eds.), *Handbook of Heterogeneous Catalysis, Vol. 4,* VCH-Verlag, Weinheim, 1997.
2. Somorjai, G. A., *Introduction to Surface Chemistry and Catalysis,* Wiley, New York, 1994.
3. Heck, R. M., and Farrauto, R. J., *Catalytic Air Pollution Control,* Wiley, New York, 1995.
4. Zhdanov, V. P., and Kasemo, B., *Surf. Sci. Rep.* 29:31 (1997) and references therein.
5. Van Hove, M. A., *Isr. J. Chem.* 38:349 (1998).
6. Somorjai, G. A., and Rupprechter, G., *J. Phys. Chem. B* 103:1623 (1999).
7. Somorjai, G. A., Su, X., McCrea, K. R., and Rider, K. B., *Top. Catal.* 8:23 (1999).
8. Cernota, P., Rider, K., Yoon, H. A., Salmeron, M., and Somorjai, G. A., *Surf. Sci.* 445:249 (2000).
9. Kung, K. Y., Chen, P., Wei, F., Shen, Y. R., and Somorjai, G. A., *Surf. Sci.* 463:627 (2000).
10. Volpp, H.-R., and Wolfrum, J., in *Applied Combustion Diagnostic* (K. Kohse-Höinghaus and J. Jeffries, eds.), Taylor & Francis, New York, 2002.
11. Härle, H., Lehnert, A., Metka, U., Volpp, H.-R., Willms, L., and Wolfrum, J., *Appl. Phys. B.* 68:567 (1999).
12. Kissel-Osterrieder, R., Behrendt, F., Warnatz, J., Metka, U., Volpp, H.-R., and Wolfrum, J., *Proc. Combust. Inst.* 28:1341 (2000).
13. Shen, Y. R., *Nature* 337:519 (1989) and references therein.
14. Härle, H., Metka, U., Volpp, H.-R., and Wolfrum, J., *Phys. Chem. Chem. Phys.* 1:5059 (1999) and references therein.
15. Bandara, A., Dobashi, S., Kubota, J., Onda, K., Wada, A., Domen, K., Hirose, C., and Kano, S. S., *Surf. Sci.* 387:312 (1997).
16. Peden, C. H. F., Goodman, D. W., Blair, D. S., Berlowitz, P. J., Fisher, G. B., and Oh, S. H., *J. Phys. Chem.* 92:1563 (1988).
17. Deutschmann, O., Behrendt, F., and Warnatz, J., *Catal. Today* 46:155 (1998).
18. Van Hove, M. A., Weinberg, W. H., and Chan, C.-M., *Low-Energy Electron Diffraction,* Springer-Verlag, Berlin, 1986.
19. Yates Jr., J. T., Thiel, P. A., and Weinberg, W. H., *Surf. Sci.* 82:45 (1979).
20. Root, T. W., Schmidt, L. D., and Fisher, G. B., *Surf. Sci.* 134:30 (1983).
21. Seebauer, E. G., Kong, A. C. F., and Schmidt, L. D., *Appl. Surf. Sci.* 31:163 (1988).
22. Hopstaken, M. J. P., and Niemantsverdriet, J. W., *J. Chem. Phys.* 113:5457 (2000).

COMMENTS

Ian Reid, BP Chemicals, UK. Given the carbon formation mechanism on Rh catalyst, are you able to comment on whether this process also occurs on platinum? Additionally can you comment on the temperature limit to maintain the catalyst with a low carbon average for Pt compared to Rh?

Author's Reply. Employing IR-VIS SFG along with postreactive AES studies, it could be demonstrated that, contrary to the general believe of surface science that CO cannot dissociate on platinum, CO does indeed dissociate on a Pt(111) single-crystal catalyst [1,2]. The major difference between the CO/Rh(111) and CO/Pt(111) adsorption system, however, is that for the CO/Rh(111) system, dissociative adsorption of CO occurs—as has been shown in the present contribution—already at room temperature, while in case of CO/Pt(111) dissociation and hence surface carbon formation starts only at a catalyst temperature above ca. 500 K at a CO pressure of 1 mbar [3].

REFERENCES

1. Kung, K. Y., Chen, P., Wei, F., Shen, Y. R., and Somorjai, G. A., *Surf. Sci.* 463:627 (2000).
2. Volpp, H.-R., and Wolfrum, J., *Applied Combustion Diagnostic* (K. Kohse-Höinghaus and J. Jeffries, eds.), Taylor & Francis, New York, 2002.
3. Metka, U., Schweitzer, M. G., Volpp, H.-R., and Wolfrum, J., unpublished data.